

Structure and Dynamics of Complexes of the Uranyl Ion with Nonamethylimidodiphosphoramidate (NIPA). 1. NMR Study of the Complex $[\text{UO}_2(\text{NIPA})_3](\text{ClO}_4)_2$

K. BOKOLO, J.-J. DELPUECH,* L. RODEHÜSER, and P. R. RUBINI

Received June 12, 1980

The $^{31}\text{P}\{^1\text{H}\}$ spectrum at -90°C of the uranyl complex ion $\text{UO}_2(\text{NIPA})_3^{2+}$, prepared as a solution of the solid perchlorate in inert anhydrous organic solvents (CH_3NO_2 , CH_2Cl_2), reveals a pentacoordinated arrangement of two symmetrically doubly bonded and one singly bonded $(\text{NMe}_2)_2\text{P}(\text{O})\text{NMeP}(\text{O})(\text{NMe}_2)_2(\text{NIPA})$ molecules about the uranyl group. A fast intramolecular exchange (for $t > -60^\circ\text{C}$) yields a full dynamic equivalence of all the phosphorus nuclei of the complex above 30°C . An intermolecular exchange between bound and free NIPA molecules is observed above 100°C upon addition of NIPA to the solutions. Both processes are independent of the amount of free NIPA. Kinetic parameters are $k(25^\circ\text{C}) = 1.3 \times 10^5$ and $3.4 \times 10^{-3} \text{ s}^{-1}$, $\Delta H^\ddagger = 11.8$ and $18.2 \text{ kcal mol}^{-1}$, and $\Delta S^\ddagger = 4.5$ and $-9.1 \text{ cal K}^{-1} \text{ mol}^{-1}$, for the intra- and intermolecular processes, respectively. These procedures are shown to proceed via a common first step, involving the breaking of a metal-ligand bond of one of the two bidentate NIPA molecules, followed by either the internal return of the tetracoordinated intermediate to the initial complex (fast) or the loss of a NIPA molecule (slow).

Introduction

Uranyl ions form important complexes with many oxygen-containing anions and neutral oxygen-containing ligands such as water, ethers, alcohols, and ketones.¹ Of special importance are uranyl complexes with organophosphorus compounds such as tributyl phosphate, which intervenes in the extraction of the uranyl nitrate from the aqueous solutions used in the extractive metallurgy of uranium. In a previous paper,² we have shown interest in using the diphosphorylated bidentate ligand nonamethylimidodiphosphoramidate (NIPA, $(\text{NMe}_2)_2\text{P}(\text{O})\text{NMeP}(\text{O})(\text{NMe}_2)_2$) which proved to be a powerful neutral chelating reagent. The purpose of this paper is to describe the NMR features of the uranyl complex $\text{UO}_2(\text{NIPA})_3^{2+}(\text{ClO}_4^-)_2$ prepared in the solid state and dissolved in an anhydrous inert solvent such as nitromethane. In fact great difficulties arose in these investigations due to the formation of several complexes, depending on the experimental conditions. To understand this, let us recall that the linear uranyl cation $\text{O}=\text{U}=\text{O}^{2+}$ can form complexes with four, five, or six donor sites displayed in the equatorial plane.³ If we examine the case of bidentate centrosymmetrical ligands L-L, a coordination number of 6 (in the equatorial plane) is unusual, because of steric factors hindering the accommodation of three ligands around the central uranyl ion. Therefore the number of coordinated ligands L-L decreases from 3 to 2. A coordination number of 6 may however be attained by the insertion of two solvent molecules (S) such as water molecules. This is the case for example with the sulfato (or nitrate) complex $\text{UO}_2(\text{SO}_4)_3^{4-}$ which, although existing in anhydrous conditions,¹ rapidly dissociates in aqueous solutions to form ions such as $\text{UO}_2(\text{SO}_4)_2(\text{H}_2\text{O})_2^{2-}$. Quite similarly, a coordination of 5 is observed with the acetylacetonato ligand (acac) which gives rise to two complexes $\text{UO}_2(\text{acac})_2\text{S}$ and $[\text{UO}_2(\text{acac})_2]_2$. In this case the coordination number increases from 4 to 5, either by the insertion of one solvent molecule (S = water, ammonia, pyridine,⁵ ethanol, or dioxane⁶) or by dimerization.⁶ In fact we observed all of these possibilities with NIPA depending on

the solvent used either in the preparation or the dissolution of the complex. This paper describes the most simple complex $\text{UO}_2(\text{NIPA})_3^{2+}$, already known in the solid state,⁷ in which no solvent molecule interferes with the NIPA ligands in the first coordination sphere. The structure of this complex as well as the dynamics of intra- and intermolecular ligand exchange were not known until now.

Experimental Section

Materials. Nonamethylimidodiphosphoramidate has been synthesized by a method described earlier.² The starting material for the synthesis of the uranyl complex was $\text{UO}_2(\text{ClO}_4)_2 \cdot x\text{H}_2\text{O}$ (Alfa Ventron). A water:uranyl ratio, x , of 6 was found by Karl Fischer titration for this compound. Distilled Fluka "puriss" grade nitromethane, vacuum rectified Fluka propylene carbonate, and Prolabo "Normapur" grade dichloromethane were used as solvents after dehydration over molecular sieves. Diethyl ether (Baker "analyzed", anhydrous) was used for synthesis.

The solid complex was synthesized in the following way. A 0.05-mol sample of $\text{UO}_2(\text{ClO}_4)_2 \cdot 6\text{H}_2\text{O}$ was dissolved in ca. 15 mL of anhydrous dichloromethane in the presence of 5 g of 3-Å molecular sieves activated shortly before. To this solution was added 0.2 mol of NIPA (i.e., an excess of 1 mol of ligand/mol of UO_2^{2+}).

The solution was stirred for several hours. The molecular sieves were replaced by the same amount of fresh ones. When dehydration was complete, the molecular sieves were filtered off and a large excess of anhydrous ether was added to the filtrate. The complex precipitated immediately. Anal. Calcd for $[\text{UO}_2(\text{NIPA})_3](\text{ClO}_4)_2$: C, 23.72; H, 5.97; N, 15.37; Cl, 5.19; P, 13.60; U, 17.41. Found: C, 23.58; H, 5.91; N, 15.21; Cl, 5.14; P, 13.63; U, 17.34. All solutions were prepared by weight. The calculated amounts of the complex salt and of the ligand (if necessary) were dissolved in nitromethane (NM), propylene carbonate (PC), or a 2:1 (v/v) mixture of dichloromethane and nitromethane (C_2N). Since the ligand and its complexes are hygroscopic, all manipulations were carried out under purified argon in a glovebox.

NMR Spectroscopy. Proton spectra were taken on a 250-MHz Cameca spectrometer or on a JEOL C60-HL apparatus working at 60 MHz, equipped with a ^{31}P broad-band decoupler (JNM SD-HC). In all cases, tetramethylsilane was used as an internal reference. Phosphorus-31 Fourier transform spectroscopy was performed on a Bruker WP-80 apparatus at 32.44 MHz (100-2000 scans of 4 K/8 K points over a frequency range of 2-5 kHz) with 85% H_3PO_4 in H_2O

- (1) Cordfunke, E. H. P. "The Chemistry of Uranium"; Elsevier: Amsterdam, 1969.
- (2) Rubini, P. R.; Rodehüser, L.; Delpuech, J.-J. *Inorg. Chem.* **1979**, *18*, 2962.
- (3) Comyns, A. E. *Chem. Rev.* **1960**, *60*, 115.
- (4) Fackler, J. P. *Prog. Inorg. Chem.* **1965**, *7*, 361.
- (5) (a) Sacconi, L.; Caroti, G.; Paoletti, P. *J. Chem. Soc.* **1958**, 4257. (b) Sacconi, L.; Giannoni, G. *Ibid.* **1954**, 2751.
- (6) Comyns, A. E.; Gatehouse, B. M.; Wait, E. J. *J. Chem. Soc.* **1958**, 4655.

- (7) Lannert, K. P.; Joesten, M. D. *Inorg. Chem.* **1968**, *7*, 2048.
- (8) (a) Lester, P. *Chem. Abstr.* **1955**, *49*, 6300g. (b) Pianka, M.; Owen, B. D. *J. Appl. Chem.* **1955**, *5*, 525. (c) Arcenaux, R. L.; Frick, J. G., Jr.; Lenard, E. K.; Reid, J. D. *J. Org. Chem.* **1959**, *24*, 1419. (d) Debo, A. *Chem. Abstr.* **1960**, *54*, 24397e. (e) De Bolster, M. W. G.; Groeneveld, W. L. *Recl. Trav. Chim. Pays-Bas* **1971**, *90*, 687; (f) DeBolster, M. W. G.; Groeneveld, W. L. *Ibid.* **1972**, *91*, 171.

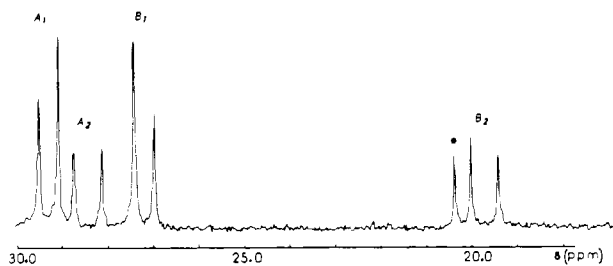


Figure 1. $^{31}\text{P}\{^1\text{H}\}$ spectrum of the complex $[\text{UO}_2(\text{NIPA})_3](\text{ClO}_4)_2$ in a 2:1 (v/v) dichloromethane–nitromethane solution at 32.44 MHz and -90°C . (A small amount of free NIPA has been added to the solution in order to give an internal reference signal, marked by an asterisk.)

Table I. Exchange Probabilities for Different Hypothetical Exchange Mechanisms^a

Scheme	$A_1B_1 \rightleftharpoons B_1A_1$	$A_1B_1 \rightarrow A_2B_2$	$A_1B_1 \rightarrow B_2A_2$	$A_2B_2 \rightleftharpoons B_2A_2$	$A_2B_2 \rightarrow A_1B_1$	$A_2B_2 \rightarrow B_1A_1$
	I	6/16	2/16	2/16	0	4/16
II	4/12	2/12	2/12	2/12	4/12	4/12
IIIa	1/2	1/2	0	0	1	0
IIIb	1/2	1/2	0	0	1	0
IIIc	1/2	0	1/2	0	0	1
IIId	1/2	0	1/2	0	0	1

^a The values given in the table represent the probabilities for one of the ligand molecules in the complex to undergo the indicated exchanges.

as an external reference and CD_3NO_2 as an internal lock substance. All ^{31}P spectra are broad band decoupled from proton. The temperature was periodically checked with a thermometer immersed in the sample tube and was found constant within $\pm 0.5^\circ\text{C}$.

Line-Shape Measurements. Two types of ligand exchange (intra- and intermolecular) are examined in this paper, the first one in the temperature range of -60 to -30°C , and the second one from 100 to 140°C . "Static" spectra, i.e., reference spectra without any line broadening due to the exchange phenomena, were performed at -80°C (^{31}P NMR) and 70°C (^1H NMR), respectively. The *intermolecular exchange* is accompanied by two NMR site exchanges, i.e., the coalescence of the two NMR signals of the bound ligand with the corresponding lines of free NIPA (cf. Figure 3b). The rate constant k_i of this exchange is the reciprocal of the mean lifetime of one bound NIPA molecule. Theoretical line shapes are computed by using a matrix formalism due to Anderson,⁹ Kubo,¹⁰ and Sack¹¹ and the program ECHGN.¹² The *intramolecular exchange* is accompanied by two to four elemental NMR site exchanges (coalescence of the four signal groups corresponding to the four nonequivalent ^{31}P nuclei: P_{A1} , P_{A2} , P_{B1} , P_{B2} (cf. Figures 1 and 2), depending on the assumed mechanism. All of them depend upon the same chemical rate constant k , i.e., the reciprocal of the mean lifetime of a given configuration of the complex, but with different exchange probabilities (Table I). Each possibility involves the same type of exchange, i.e., the exchange of an AB type quadruplet with another AB type quadruplet, which may be identical with or different from the first one. In the latter case, the intensity ratio between the two multiplets is 2:1. The four elemental NMR site exchanges are of the following type (for notation, see below): $A_1B_1 \rightleftharpoons B_1A_1$, $A_1B_1 \rightleftharpoons A_2B_2$, $A_1B_1 \rightleftharpoons B_2A_2$, $A_2B_2 \rightleftharpoons B_2A_2$. Theoretical line shapes were computed by using a density matrix formalism and a single program EXCH14.¹⁴ This program permitted the necessary computations for each elemental exchange (of the general type $\text{AB} \rightleftharpoons \text{A'B'}$) by introducing the appropriate NMR parameters; the data thus obtained were then automatically summed up with use

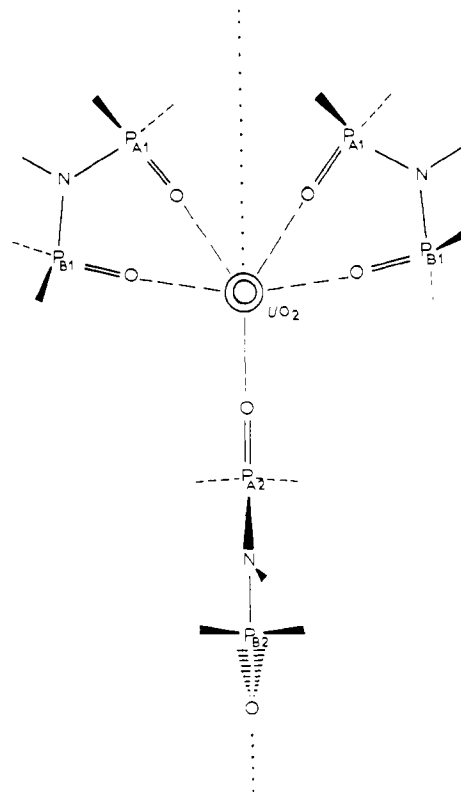


Figure 2. Structure proposed for the complex ion $\text{UO}_2(\text{NIPA})_3^{2+}$ in solution. The figure shows a projection on the equatorial plane, perpendicular to the axis $\text{O}=\text{U}=\text{O}$ of the UO_2^{2+} ion and passing through the uranium(VI) atom. The trace of the vertical plane of symmetry (a C_2 axis) is shown by a dotted line.

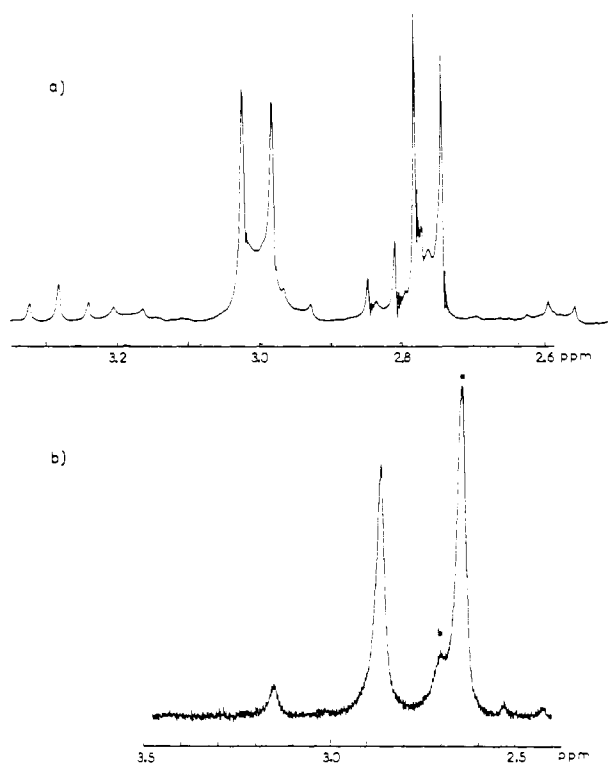


Figure 3. (a) 250-MHz proton spectrum of NIPA and the uranyl complex in nitromethane at 25°C . (b) The same spectrum at 60 MHz, broad band decoupled from ^{31}P .

- (9) Anderson, P. W. *J. Phys. Soc. Jpn.* **1954**, *9*, 316.
 (10) Kubo, R. *J. Phys. Soc. Jpn.* **1954**, *9*, 935.
 (11) Sack, R. A. *Mol. Phys.* **1958**, *1*, 163.
 (12) Martin, M. L.; Delpuech, J.-J.; Martin, G. J. "Practical NMR Spectroscopy"; Heyden: London, 1979; pp 441–444.
 (13) (a) Kaplan, J. J. *J. Chem. Phys.* **1958**, *28*, 278; **1958**, *29*, 462. (b) Alexander, S. J. *J. Chem. Phys.* **1962**, *37*, 967.
 (14) (a) Delpuech, J.-J. *Mol. Phys.* **1968**, *14*, 567. (b) Delpuech, J.-J.; Serratrice, G. *Org. Magn. Reson.* **1972**, *4*, 667.

of the weighting factors of Table I. Rate constants k were adjusted by trial and error so as to obtain the best fit of the theoretical to the experimental curves, with use of successively the six possible sets of

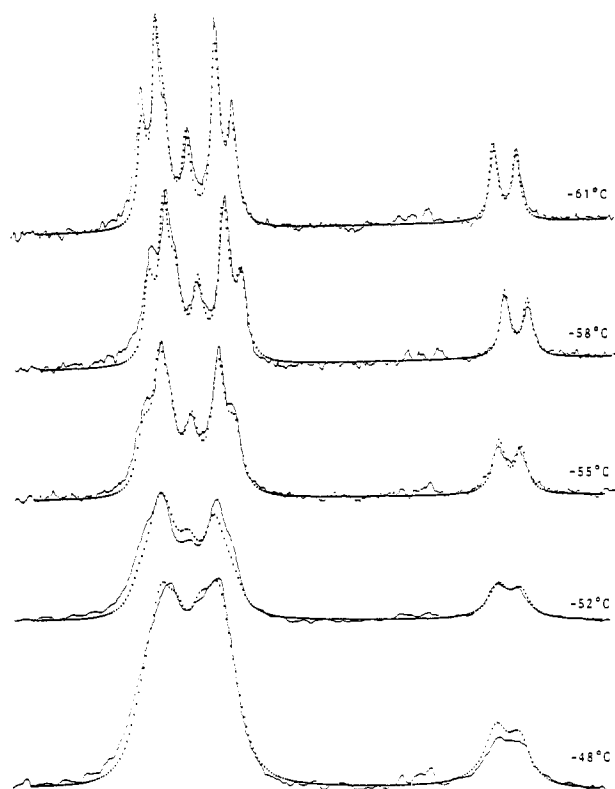


Figure 4. Experimental and theoretical curves for the $^{31}\text{P}\{^1\text{H}\}$ site exchange at 32.44 MHz and different temperatures in a 2:1 (v/v) dichloromethane–nitromethane solution. (Solid lines are the experimental spectra; dotted lines represent the theoretical curves calculated on the basis of Scheme I).

weighting factors of Table I. In fact only the first set yielded a good fit. This points to the predominance of Scheme I for the intramolecular rearrangement (Figure 4). All calculations were performed with use of a Texas Instruments 980A minicomputer equipped with a digital plotter Hewlett-Packard 7210A.

Results and Discussion

Structure of the Complex. At room temperature, the $^{31}\text{P}\{^1\text{H}\}$ spectrum of a solution of the solid complex $\text{UO}_2(\text{NIPA})_3^{2+}$ consists of a single line shifted by 8.0 ppm downfield from the signal of free NIPA at 20.4 ppm (reference: 85% H_3PO_4). This singlet actually results from the coalescence of a more complex spectrum which can be observed at lower temperatures when the intramolecular motion of the ligand molecules is slow on the NMR time scale. At -90°C we observed a splitting of the singlet into two AB patterns, A_1B_1 and A_2B_2 as shown in Figure 1. The first set of signals (A_1B_1) is more intense than the second one (A_2B_2); the intensity ratio has a value of 2:1 and is found to be independent of the salt concentration. The intensities of the two sets correspond to two and one NIPA molecules, respectively. The absence of perchlorate ions in the first solvation shell of the UO_2^{2+} cation is shown by the fact that no splitting of the IR absorption line of the perchlorate ion at 616 cm^{-1} could be detected. As pointed out by De Bolster et al.^{8f} and Airoidi et al.²³ the coordination of the ClO_4^- anion would lead to a lowering of T_d to C_{3v} or C_{2v} symmetry, resulting in the splitting of the IR absorptions. The molar conductance value of $174\text{ cm}^2\ \Omega^{-1}\ \text{mol}^{-1}$ found for solutions of the complex in nitromethane corresponds to the conductance range ($130\text{--}180\text{ cm}^2\ \Omega^{-1}\ \text{mol}^{-1}$) usually observed for 2:1 electrolytes in this solvent and is very close to that given by Lannert and Joesten.⁷ All these observations prove that the complex is completely dissociated in solution.

This clearly shows the presence of one uranyl complex in solution still containing three coordinated NIPA molecules. However, the simultaneous binding of all three molecules in the same way would lead to a configuration of higher symmetry (e.g., C_{3v}) than that actually observed. The chemical shifts for all phosphorus atoms would be identical, in sharp contrast with the existence of four different sites as revealed by the ^{31}P spectrum. The existence of the two AB patterns led us to divide the three coordinated NIPA ligands into two subsets 1 and 2 of two and one molecules, corresponding to the A_1B_1 and A_2B_2 parts of the spectrum, respectively. Within each subset the two phosphorus nuclei of any one NIPA molecule are not equivalent; however, the two NIPA molecules, (i.e., 1 and 1') of the first subset are equivalent: this shows the existence of a symmetry element in the structure of the complex uranyl ion *exchanging the two nonequivalent nuclei* ($\text{P}_{\text{A}1}$, $\text{P}_{\text{B}1}$) of the first NIPA ligand with those ($\text{P}_{\text{A}'1}$, $\text{P}_{\text{B}'1}$) of the second one within the first subset and *leaving unchanged the single NIPA molecule* ($\text{P}_{\text{A}2}$, $\text{P}_{\text{B}2}$) of the second subset. From these observations we conclude the existence of two bidentate and one monodentate NIPA molecules in the complex ion (Figure 2), resulting in a pentagonal-bipyramidal arrangement of oxygens about the uranium(VI). The crystal structures of NIPA complexes have not been described to date. However they are reported to be isomorphous¹⁵ with the octamethylpyrophosphoramidate complexes of known structure,^{7,16} so that we may reasonably assume the planarity of the chelate rings (bidentate NIPA ligands) and the coplanarity of the chelate rings with the uranium(VI) atom. The pentagon formed by the five donor oxygen atoms may assume either a planar or a puckered configuration; i.e., the two chelate rings may be either coplanar with or equally inclined with respect to the equatorial plane. In the first event, the complex has a C_{2v} symmetry, with two perpendicular planes intersecting along the C_2 axis, the equatorial plane and the plane π containing the uranyl $\text{O}=\text{U}=\text{O}$ unit and the $\text{P}_{\text{A}2}\text{P}_{\text{B}2}$ phosphorus atoms.¹⁷ In the second case the complex may possess either the C_2 or the π -symmetry element alone which can account for all the observations cited above.

There are two further pieces of evidence supporting the assumed structure of the complex.

(a) The B_2 signals appear at 19.71 ppm, quite apart from the rest of the spectrum, and close to the resonance of free NIPA (20.4 ppm), whereas the corresponding A_2 resonance (28.33 ppm) lies within the frequency range of the A_1B_1 pattern (27.09–29.15 ppm). This shows that B_2 signals correspond to the uncoordinated phosphoryl group of the monodentate NIPA molecule, whereas A_1B_1 and A_2 signals refer to the coordinated $\text{P}=\text{O}$ groups in the bidentate and monodentate ligands.

(b) The $^{31}\text{P}\text{--}^{31}\text{P}$ coupling constant of the A_2B_2 part of the spectrum (22.0 Hz) is larger than that of the A_1B_1 case (15.6 Hz), suggesting a conformation of the corresponding molecule different from that of the other two ligand molecules.

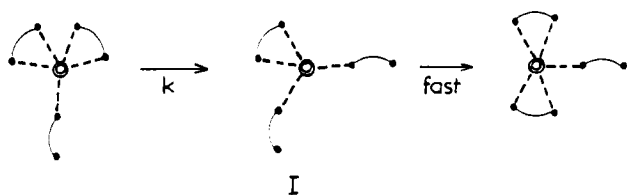
These conclusions are nicely confirmed by our results from proton spectroscopy. The ^1H NMR spectrum of pure NIPA cannot be analyzed simply by assuming first-order couplings between the phosphorus nuclei and the immediately adjacent *N*-methyl protons, i.e., as a doublet for the terminal and a triplet for the bridging *N*-methyl protons. The expected lines are indeed observed but are broadened as a result of second-order effects due to long-range couplings $^5J_{\text{P}\text{--}\text{H}}$ (Figure 3a).

(15) Miller, P. T.; Lenhart, P. G.; Joesten, M. D. *Inorg. Chem.* **1972**, *11*, 2221.

(16) Joesten, M. D.; Hussain, M. S.; Lenhart, P. G. *Inorg. Chem.* **1970**, *9*, 151 and references cited therein.

(17) In fact, the plane of the singly bonded NIPA molecule may internally rotate about the $\text{P}_{\text{A}2}=\text{O}\cdots\text{U}^{\text{VI}}$ bond, and the axial symmetry about the $\text{O}=\text{P}_{\text{A}2}$ segment may result from a dynamical average.

Scheme I



This phenomenon is suppressed by decoupling the phosphorus nuclei, so that the ^1H spectrum is reduced to two sharp singlets a and b at 2.66 and 2.71 ppm, the ratio of their intensities being 8:1 as expected from the 24 and 3 protons of the terminal and the bridging *N*-methyl protons, respectively (Figure 3b). At low temperature (-90°C) the 250-MHz proton spectrum of the complex exhibits the line multiplicity and the intensity ratios expected from the presence of both bidentate and monodentate NIPA molecules. The multiplets corresponding to the terminal *N*-methyl substituents on the P_{A_1} atom are shifted by 0.02 ppm from those on P_{B_1} . The terminal *N*-methyl groups on P_{A_2} and P_{B_2} appear at 2.93 and 2.76 ppm, respectively. The bridging *N*-methyl group of the monodentate molecule is shifted by 0.185 ppm downfield from that of the bidentate NIPA molecules and appears at 3.19 ppm. These results agree perfectly with the conclusions drawn from the less complicated ^{31}P spectrum.

As mentioned above, uranyl complexes containing two bulky bidentate ligands may complete their coordination number to 5 (or 6) by the insertion of one (or two) smaller monodentate molecules. In this respect, single-crystal X-ray crystallography has effectively revealed a pentagonal-bipyramidal arrangement in the complex $\text{UO}_2(\text{acac})_2\text{H}_2\text{O}$.¹⁸ However, in the case of the complex ion $\text{UO}_2(\text{NIPA})_3^{2+}$, we are dealing with the interesting new situation that the additional monodentate ligand is in fact a singly bonded bidentate molecule identical with the other two doubly bonded NIPA molecules. This result may be of interest for the study or reexamination of other uranyl complexes containing three bidentate ligands.

Such a structure, however, is very labile due to the presence of the free reactive end of the singly bonded NIPA molecule and can give rise to two types of exchange: a fast intramolecular exchange observed at temperatures between -60 and -30°C and a much slower intermolecular exchange (upon addition of variable amounts of free NIPA, at 100 – 140°C). The mechanisms and kinetics of these exchanges are examined in the following.

Low-Temperature NMR Site Exchange. The coalescence of both ^{31}P and ^1H lines in the temperature range between -90 and -30°C was assigned to an intramolecular exchange of singly and doubly bonded NIPA molecules for the following reasons: (a) the site exchange occurs even in the absence of any free NIPA added to a solution of the solid complex; (b) one coalescence occurs at 100 – 140°C between signals of bound and free NIPA; (c) the low-temperature exchange is independent of the concentrations of both the ligand and the added free NIPA.

Basically there are three possible kinds of mechanism for these kinetics.

(i) The first possibility is a reaction proceeding via a hexacoordinated transition state (I) in which two NIPA molecules are singly bonded to the central uranium(VI) (Scheme I).

Scheme II

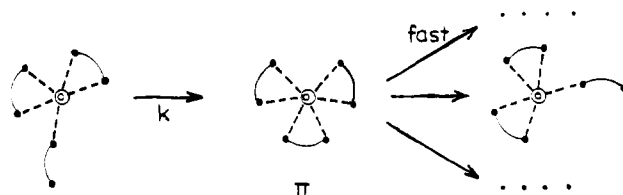
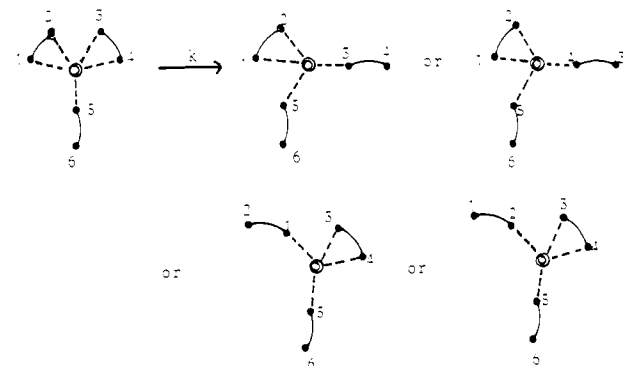


Table II. Experimental Rate Constants for the Intramolecular Rearrangement of the Ligands in the Complex $[\text{UO}_2(\text{NIPA})_3](\text{ClO}_4)_2$ as a Function of Temperature

$t, ^\circ\text{C}$	k, s^{-1}	$t, ^\circ\text{C}$	k, s^{-1}
-38	450 ± 50	-55	55 ± 5
-45	250 ± 20	-58	38 ± 3
-48	130 ± 15	-61	28.5 ± 3
-52	90 ± 10		

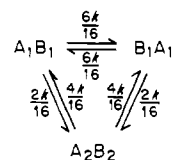
From an initial configuration there are four possibilities for attaining the transition state depending on which end of either of the two bidentate ligand detaches.



From each transition state, there are four possible recombinations depending on which side a monodentate ligand attaches.

For one initially bidentate molecule, there are six exchanges $\text{A}_1\text{B}_1 \rightarrow \text{B}_1\text{A}_1$ with a rate of $6k/16$, two exchanges $\text{A}_1\text{B}_1 \rightarrow \text{A}_2\text{B}_2$ with a rate of $2k/16$, and two exchanges $\text{A}_1\text{B}_1 \rightarrow \text{B}_2\text{A}_2$ with a rate of $2k/16$.

For the monodentate ligand, there are four exchanges $\text{A}_2\text{B}_2 \rightarrow \text{A}_1\text{B}_1$ with a rate of $4k/16$ and four exchanges $\text{A}_2\text{B}_2 \rightarrow \text{B}_1\text{A}_1$ with a rate of $4k/16$. The exchange for any one of the ligands following Scheme I can therefore be resumed in the scheme



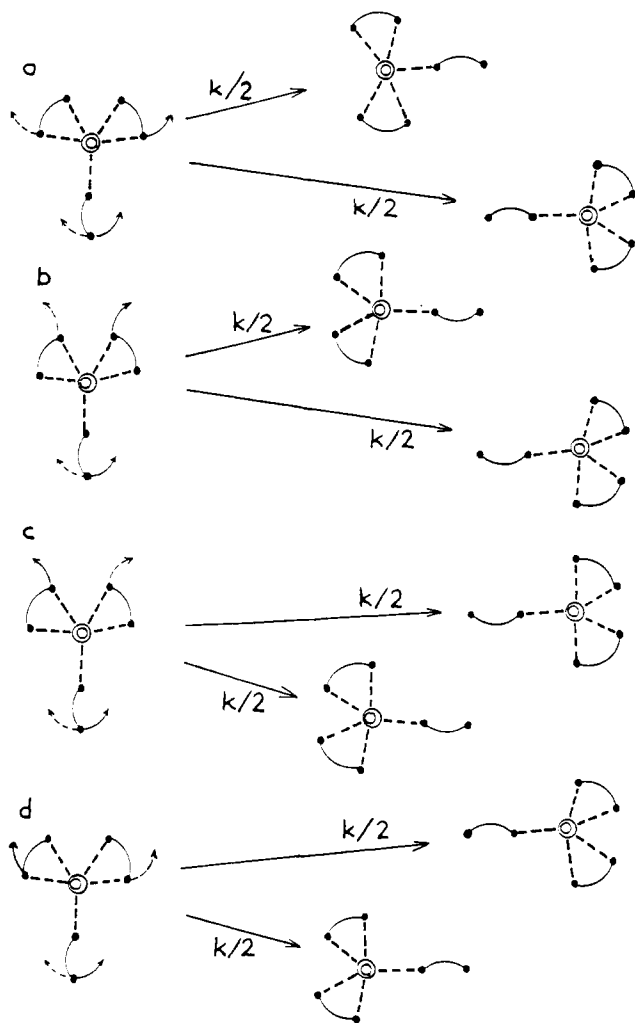
As evident from the structure of the complex the two bidentate NIPA molecules correspond to the A_1B_1 NMR sites and the monodentate ligand to the A_2B_2 sites. The relative populations are therefore $P_{\text{A}_1\text{B}_1} = 2/3$ and $P_{\text{A}_2\text{B}_2} = 1/3$.

The ratio of these populations has to be taken into account for calculating the exchange probabilities for the entire complex. The probabilities for the different exchanges with respect to one ligand molecule are summarized in Table I.

(ii) A second mechanism implies a symmetric octacoordinate transition state (II, Scheme II) with subsequent detachment of one of the six $\text{P}=\text{O}$ groups. The results for the possibilities of exchange obtained by a treatment analogous to that for Scheme I are given in Table I.

(18) Frasson, E.; Bombieri, G.; Panattoni, C. *Nature (London)* **1964**, *202*, 1325.

Scheme III



(iii) The third reaction pathway accounts for the synchronous formation and rupture of the U \cdots O=P bonds. The reaction scheme is complicated by the fact that any of the coordinated phosphoryl groups may leave the inner sphere on attack of the "free" group. Depending on the initial position of the leaving group we discern four subschemes (see Scheme III). The respective probabilities for this mechanism are also summarized in Table I.

The calculations of the theoretical spectra corresponding to each of these cases and comparison with the experimental results allowed us to prove that Scheme I represents the most probable mechanism for the intramolecular rearrangement observed (Figure 4). The values obtained for the first-order rate constant k at seven temperatures are shown in Table II. Only the less complicated ^{31}P spectra were used for this purpose.

From the variation of k with temperature, the activation parameters of the rearrangement have been calculated. The corresponding values are $\Delta H^\ddagger = 11.8 \pm 0.4 \text{ kcal mol}^{-1}$, $\Delta S^\ddagger = 4.5 \pm 1.2 \text{ cal K}^{-1} \text{ mol}^{-1}$, and $k(25^\circ\text{C}) = 1.3 \times 10^5 \text{ s}^{-1}$.

The slightly positive value of ΔS^\ddagger is in agreement with the detachment of a P=O group in a dissociative mode according to Scheme I. The relatively high activation enthalpy is consistent with the rupture of a strong uranium(VI)–phosphoryl bond.

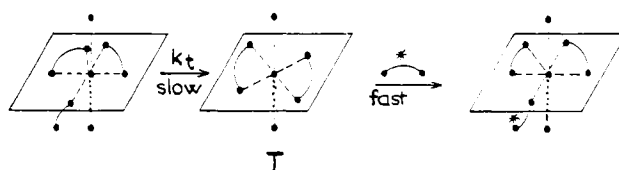
Intermolecular Ligand Exchange. Upon addition of free NIPA to a solution of the complex $[\text{UO}_2(\text{NIPA})_3](\text{ClO}_4)_2$, ligand exchange between bound and noncoordinated ("free") NIPA occurs at temperatures above ca. 100°C on the NMR time scale. This process is observed by ^1H NMR as an ex-

Table III. Rate Constants and Activation Parameters for the

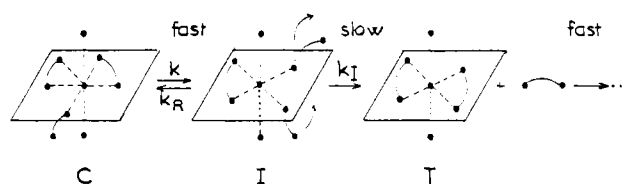
$t, ^\circ\text{C}$	k_t, s^{-1}			
	a	b	c	d
102	2.1	1.9		
108	2.8	3.1		
110			3.6	3.5
116	4.3	4.7		
122			7.5	7.6
123	7.5	8.0		
129	13.0	12.0		
130			10.5	10.0
135			15.0	
136	18.0	17.0		13.0
142			21.0	24.0
$\Delta H_t^\ddagger, \text{e kcal mol}^{-1}$	19.6	19.2	16.6	17.3
$\Delta S_t^\ddagger, \text{cal mol}^{-1} \text{K}^{-1}$	-5.6	-6.3	-13.2	-11.3
$\Delta G_t^\ddagger, \text{kcal mol}^{-1}$	21.2	21.1	20.5	20.7

^a At $C_{\text{complex}} = 0.0244 \text{ M}$ and $C_{\text{ligand}} = 0.0800 \text{ M}$. ^b At $C_{\text{complex}} = 0.0253 \text{ M}$ and $C_{\text{ligand}} = 0.0499 \text{ M}$. ^c At $C_{\text{complex}} = 0.0490 \text{ M}$ and $C_{\text{ligand}} = 0.1602 \text{ M}$. ^d At $C_{\text{complex}} = 0.0977 \text{ M}$ and $C_{\text{ligand}} = 0.3204 \text{ M}$. ^e Mean values of the activation parameters are $\Delta H_t^\ddagger = 18.2 \pm 1.2 \text{ kcal mol}^{-1}$, $\Delta S_t^\ddagger = -9.1 \pm 3.1 \text{ cal mol}^{-1} \text{K}^{-1}$, and $\Delta G_t^\ddagger = 20.9 \pm 0.3 \text{ kcal mol}^{-1}$.

Scheme IV



Scheme V



change between the sites for bound (S_b) and free (S_f) ligand giving separate signals at lower temperatures ($<70^\circ\text{C}$) (Figure 3b); see eq 1. For the studies above 70°C , propylene car-



bonate has been used as a solvent instead of nitromethane, since its boiling point is higher and its solvation characteristics are similar to those of nitromethane.

Kinetic measurements by the dynamic NMR technique were made (observing the proton signals decoupled from ^{31}P at five to six different temperatures) on solutions containing variable amounts of complex and free ligand (Table III).

The exchange rate is found to be independent of the concentration of free NIPA as well as of the salt concentration; i.e., the kinetic order of the exchange reaction with respect to free ligand is zero. The activation parameters calculated from the rate constants k_t reported in Table III are $\Delta H_t^\ddagger = 18.2 \pm 1.2 \text{ kcal mol}^{-1}$, $\Delta S_t^\ddagger = -9.1 \pm 3.1 \text{ cal K}^{-1} \text{ mol}^{-1}$, and $k_t(25^\circ\text{C}) = 3.4 \times 10^{-3} \text{ s}^{-1}$.

Mechanism of the Exchange Reaction. Since the concentration of the free ligand has no influence on the rate of exchange, the mechanism of the reaction is supposed to have a dissociative character, thus involving a hexacoordinated intermediate (T), as tentatively shown in Schemes IV and V.

Scheme IV involves the detachment of the single-bonded NIPA ligand as the rate-determining step. The exchange

reaction is completed by a fast reattachment of another NIPA molecule from the bulk of the solution (NIPA*).

This mechanism, however, is not compatible with the negative value of the activation entropy. One would rather expect a positive value of ΔS_i^\ddagger for a transition state with fewer molecules coordinated to the uranium atom than in the ground state.

Another mechanism is therefore proposed (Scheme V) in which the loss of a coordinated ligand proceeds in two steps. The first step is assumed to be identical with the one discussed for the intramolecular ligand exchange described above and yields a hexacoordinated intermediate (I) still containing three NIPA molecules as described in Scheme I. This intermediate would in a second step either rearrange to the initial hepta-coordinated complex C (rate constant k_R) or loose a singly bonded NIPA molecule to give the hexacoordinated intermediate T (rate constant k_I). In the latter case, the exchange reaction would be quickly completed by the reactions $T + \text{NIPA}^* \rightarrow I \rightarrow C$. The detachment of one of the two singly bonded NIPA molecules and the reattachment of the free extremity of the other one in the reaction $I \rightarrow T$ are assumed to occur synchronously. This internally assisted ligand displacement, quite analogous to an internal nucleophilic substitution about a saturated carbon atom, would lead to a lower activation enthalpy and be accompanied by an entropy change of uncertain sign, thus accounting for the moderately high activation enthalpy and the slightly negative entropy of the whole process.

The first step of Scheme V thus implies the rupture of a uranyl O=P bond without a dissociation of a ligand molecule leading to an intermediate containing still three NIPA molecules.

In contrast, the intermediate (T) of Scheme IV is formed by the complete dissociation of the monodentate ligand.

Consequently the internal substitution step characterized by k_I is assumed to be slower than the initial step leading from C to I.

Under these conditions, the apparent first-order rate constant observed, k_t , may actually be written as eq 2. At 25

$$k_t = \frac{k k_I}{k_I + k_R} = \frac{k k_I}{k_R} \quad (2)$$

°C, k and k_I are equal to 1.3×10^5 and $3.4 \times 10^{-3} \text{ s}^{-1}$, and therefore $k_R/k_I = 3.8 \times 10^7$. This means that the internal

return of I to C proceeds ca. 10^7 times faster than the ligand detachment in the reaction $I \rightarrow T$. The differences between the activation parameters of these two concurrent processes may be simply computed as eq 3 and 4.

$$\Delta H_I^\ddagger - \Delta H_R^\ddagger = \Delta H_I^\ddagger - \Delta H^\ddagger = 6.4 \text{ kcal mol}^{-1} \quad (3)$$

$$\Delta S_I^\ddagger - \Delta S_R^\ddagger = \Delta S_I^\ddagger - \Delta S^\ddagger = -13.6 \text{ cal K}^{-1} \text{ mol}^{-1} \quad (4)$$

These exchanges exhibit some analogies with those previously described² for NIPA complexes having a much more classical structure. We observed both an intramolecular rearrangement and an intermolecular ligand exchange in D_3 tris-chelated NIPA complexes, involving the detachment of one end of the chelate as a common first step. In this respect, the kinetic parameters for the uranyl complex are not very different from those obtained for the magnesium complex $\text{Mg}(\text{NIPA})_3^{2+}$ ($k_t(25^\circ\text{C}) = 4.3 \times 10^{-2} \text{ s}^{-1}$, $\Delta H_t^\ddagger = 15.7 \text{ kcal mol}^{-1}$, and $\Delta S_t^\ddagger = -11.9 \text{ cal K}^{-1} \text{ mol}^{-1}$).

In the literature, information on the symmetrical substitution of bidentate ligands around metal ions is very limited.^{19,20} As far as the uranyl ion is concerned, ligand-exchange studies seem to be restricted to the bis(acetylacetonato) chelates.^{21,22} The intermolecular exchange proceeds in this case via both a unimolecular and a bimolecular process.²² The second process is assumed to involve an intermediate with an increased coordination number, presumably a heptacoordinated intermediate. This contrasts with the exceptional stability of the analogous heptacoordinated NIPA complex, which is observed as a long-lived species in solution, in spite of a larger steric hindrance and a zero electrical charge of the NIPA ligand molecules. Further studies on heptacoordinated complexes of uranium(VI) of the general type $\text{UO}_2(\text{NIPA})_2\text{S}^{2+}$ (cf. Introduction) are in progress.

Acknowledgment. We thank the Centre National de la Recherche Scientifique for support. All NMR spectra were recorded on spectrometers of the Groupement Régional de Mesures Physiques de l'Académie de Nancy-Metz. We thank Mr. Dumortier and Mrs. Eppiger for their technical assistance.

Registry No. $[\text{UO}_2(\text{NIPA})_3](\text{ClO}_4)_2$, 21793-18-0.

(19) Pearson, R. G.; Lanier, R. D. *J. Am. Chem. Soc.* **1964**, *86*, 765.

(20) Chatterjee, C.; Matsuzawa, K.; Kido, H.; Saito, K. *Bull. Chem. Soc. Jpn.* **1974**, *47*, 2809.

(21) Vasilescu, A. *Rev. Roum. Chim.* **1975**, *20*, 951.

(22) Vasilescu, A.; Oncescu, T. *Rev. Roum. Chim.* **1978**, *23*, 1055.

(23) Airoldi, C.; Gushikem, Y.; Puschel, C. R. *J. Coord. Chem.* **1976**, *6*, 17.